

Applied Element Simulation for Collapse Analysis of Structures

by

Hatem Tagel-Din* and Kimiro Meguro**

ABSTRACT

A new extension for the Applied Element Method (AEM) for structural analysis is introduced. This paper introduces a numerical approach to deal with detailed structural collapse process. Contact and collision forces are considered in the analysis through collision springs, which are added at the locations where collision or recontact between elements occurs. The effects of separation, recontact and collision can be considered easily with high accuracy and without large increase of the CPU time. The main advantage of the proposed technique compared to the Extended Distinct Element Method (EDEM) is that the time increment can be much larger than the EDEM.

INTRODUCTION

Applied Element Method (AEM) is a newly developed method for structural analysis. The main advantage of the method is that it can follow the structural behavior since the application of load, crack initiation and propagation, separation of structural elements and till total collapse in reasonable time with reliable accuracy. The applicability and accuracy of the AEM in various fields of applications were discussed in many previous publications¹⁾⁻⁵⁾. It was proved that the method can follow crack initiation, propagation and load deformation till failure in Ref. (1). The complicated process of crack opening and crack closure could be also followed¹⁾. It was proved also that the crack initiation and propagation direction does not depend on element shape or arrangement²⁾. Even the effects of Poisson's ratio, which normally neglected in the discrete type model, could be considered³⁾. The rigid body motion of failed structural elements could be simulated accurately⁴⁾. In addition, it was proved that the method can follow buckling load, mode and post-buckling behavior in reasonable CPU time and reliable accuracy⁵⁾.

The only limitation in the analysis till this stage is the representation of collision and recontact between failed structural elements during collapse. However, collision and recontact problems are essential in many cases. For example, "What is the effect of collision between falling structural elements and neighbor structures", "What happens if structures having different dynamic characteristics collide during earthquakes", "If a structure collapse, where and how do they undergo collapse" and "What is the time of collapse". These questions can not be answered unless the numerical technique considers the collision effects.

Although, these effects are very important from the viewpoint of safety and/or security of users, only few numerical techniques can deal with these problems. Many analyses for collision problems were performed using the EDEM^{6), 7)}. However, as the simulation using the EDEM needs long CPU time and it is less accurate than the proposed method in small deformation range, it is better to extend the newly developed method to deal with the collision problems. Other methods like Discontinuous Deformation Analysis, DDA⁸⁾, were applied for large deformation of rocks. The applicability of the DDA is still limited to simulation of behavior of rocks or bricks. In addition, the method requires long CPU time and big experiences to perform the simulation and in many cases, algorithm is not stable⁸⁾.

* Ph.D., visiting researcher, Institute of Industrial Science, The University of Tokyo

** Associate Professor, International Center for Disaster-Mitigation Engineering, Institute of Industrial Science, The University of Tokyo

This paper introduces the numerical technique to deal with collision problems. The results are compared with the theoretical ones showing good accuracy. The results of failure process of structures are also introduced. It is proved through these analyses that the proposed method can analyze structural behavior during collapse, even during collision with other structures and/or with the ground within reasonable CPU time with reliable accuracy. As the first step of the research, simple models for concrete, steel and cut of reinforcement are used and these are approximate. For future study of the detailed collapse mechanism of structures, additional effects like buckling of reinforcement bars, separation of concrete cover, compression shear failure and strain rate effect on material properties are needed to be modeled as they are not taken into account in the model yet.

NUMERICAL REPRESENTATION OF COLLISION AND RECONTACT

To consider the effects of collision, it is necessary to check the collision between elements during analysis. To simplify the problem, element shape is assumed as circle during collision. This assumption is acceptable if the element size is relatively small. Even in case of relatively large elements used, it may be reasonable because in the deformation range of collision, the sharp corners of elements are broken due to the stress concentration and the edge of the elements become round shape. Based on the assumptions, only distance between the centres of the elements is calculated to check collision. This process takes longer time if the element shape is irregular.

Checking collision between an element and all the other elements takes long CPU time. This time is proportional to $(N \times N)$, where N is the number of elements. To overcome this problem, the geometrical coordinates technique is adopted. Using this technique, the studied space is divided into grids of proper size. Every elements has its space coordinates that depends on its location during analysis. These coordinates change during analysis especially after failure due to large geometrical changes in the structure. Using this technique, contact between elements is checked between the element and its neighbor elements only, instead of all elements, which saves CPU time.

The following technique is used for representation of collision:

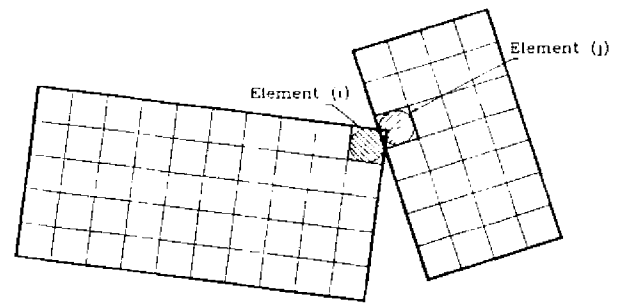
1. Solve Eq. (1) for static loads, like gravity loads, and get the displacements.
2. Select a proper value for initial time increment. Before collision occurs, relatively long time increments can be used and its value depends mainly on the case studied.

$$[K_m][\Delta U] = \Delta F_s \quad (1)$$

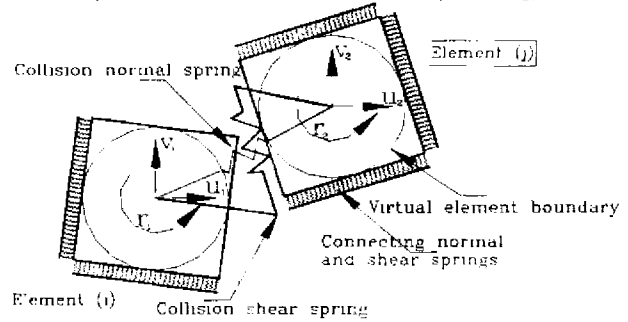
Where $[K_m]$ is the nonlinear stiffness matrix; ΔF_s the incremental static load vector; $[\Delta U]$ the incremental displacement vector. It should be emphasized that Eq. (1) can not be solved if the studied phenomenon is originally unstable, like case of falling object on a structure.

3. Solve the Eq. (2) using Newmark Beta technique⁹⁾ and get the displacements

$$[M][\Delta \ddot{U}] + [C][\Delta \dot{U}] + [K_m][\Delta U] = \Delta f(t) \quad (2)$$



a) Collision between elements (i) and (j)



b) Close up of the elements in collision process

Fig. (1) Collision normal and shear springs

Where $[M]$ is mass matrix; $[C]$ the damping matrix; $\Delta f(t)$ the incremental applied load vector; and $[\Delta \dot{U}]$ and $[\Delta \ddot{U}]$ the incremental velocity and acceleration vectors, respectively.

4. Modify the structure geometry by modifying the element position and orientation according to the calculated displacements.
5. Modify the direction of spring forces according to the new geometry.
6. Calculate the element geometrical coordinates corresponding to each element.
7. Check for collision between each element and its neighbours. If collision occurs, do the followings:
 - The time increment should be reduced to follow the material behavior properly during collision. This value depends on many factors, like relative velocity between elements before collision and force transmitted during contact and it should be selected properly. If, for example, force between contact elements are very small, like in case of elements moving nearly with slightly different velocities, longer time increment can be used. Generally, the time increment during transmission of collision forces should be less than the contact time between elements. After separation of elements, the time increment is increased automatically by the program to its initial values.
 - Add collision springs, normal and shear springs, between collide two elements, refer to Fig. (1). The normal spring direction passes through the elements centroid, while shear spring direction is tangent to the assumed entire circles. These springs exist if the elements are in contact and removed after separation of elements. When elements separate, residual tension and shear forces are redistributed by applying the forces in the reverse directions.
 - The global stiffness matrix, which is of sparse type⁽¹⁰⁾, is assembled in a vector form. This vector consists of the non-zero elements of half of the original matrix. Using this technique, band width associated for each degree of freedom depends mainly on element contacts. Having minimum difference between elements numbering results in a small-sized sparse matrix and hence, short CPU analysis time becomes possible. If element contacts do not change, the band width associated for each degree of freedom is constant and this saves CPU time, as the location of each stiffness matrix element is determined just once before the analysis. After collision occurrence, the sparse stiffness matrix is modified as follows:
 - A. The bandwidth associated with the elements in contact is determined. This bandwidth increases because of existence of new contacts. This increase depends mainly on the difference in numbering between the element and new contacted elements.
 - B. The new position of element stiffness matrix in the global vector is recalculated due to the increase of the bandwidth. This leads to increasing the global vector size and the CPU time required for analysis.
 - C. The new bandwidth calculated for each degree of freedom is used in following increments till new contacts occur.
 - Set collision spring stiffness equal to zero and make redistribution of residual tension forces if separation occurs.
8. Determine the resultant spring forces, including forces from collision springs, at the location of each element centroid $\{F_m\}$.
9. Determine the geometrical residuals by:

$$F_G = f(t) - [M][\ddot{U}] - [C][\dot{U}] - F_m \quad (3)$$

10. Determine the new stiffness matrix for the new configuration

$$[M][\Delta \ddot{U}] + [C][\Delta \dot{U}] + [K_m][\Delta U] = \Delta f(t) + F_G \quad (4)$$

11. Solve Eq. (4) and calculate incremental displacement, velocity and acceleration for each element.
12. Apply new time increment and go to step (4)

In case of earthquake ground acceleration, the term $\Delta f(t)$ is replaced by the incremental ground acceleration matrix ($-m\Delta\ddot{u}_g$).

It should be emphasized that the adopted time increment should fulfill the followings:

1. Before collision, incremental geometrical changes of the structure compared to the structure dimensions should be small enough as small deformation theory is adopted during each time increment.
2. After contact, using large time increments leads to excessive overlapping between elements, which usually leads to some numerical errors.

MATERIAL MODELING

a) Modeling of distributed springs

As the collapse phenomenon is a very complicated phenomenon, which can not be solved in two dimensional model, some assumptions are adopted to simplify the analysis. The main assumptions in material modeling of distributed springs are:

1. Although the fracture process of concrete or steel spring should take a specific time, this effect is neglected and the total value of the failed spring force is redistributed in the following time increment. No tension softening is permitted.
2. Effects of pull out and buckling of reinforcement bars, which occurs at large strain levels, are not considered. This is due to the approximation that both the reinforcement bar and the attached element have the same degrees of freedom.
3. In static analysis, minimum stiffness value can be assumed for concrete springs after cracking. This results in having residual tension force acting at the normal springs after cracking which is redistributed in the next increment. However, this technique can not be applied in dynamic analysis case. Assuming minimum stiffness value at the crack location affects the dynamic behavior of elements after separation of structural elements. For example, rigid body motion of elements can not be followed accurately if minimum stiffness value is assumed. Hence, spring stiffness after cracking is assumed zero till the crack closure occurs.
4. After reaching 1.0 % strain in concrete, compression springs are not allowed to fail. This assumption is adopted mainly to prevent overlapping between elements after collision.
5. Effect of strain rate in the compressive and tensile resistance of the material is neglected. For more details about concrete behavior under impulsive loading, refer to Refs. (12) and (13).
6. When distance between element centers reaches a specific large value, distributed springs between these elements are removed and hence, elements are assumed separated. Recontact between these elements occurs as circles and material models applied are illustrated in the next section.

The aforementioned assumptions are adopted just to simplify the analysis. It should be emphasized that more complicated accurate models can be adopted in the analysis.

b) Modeling of contact springs

When elements collide, new springs called collision springs are added between the collide elements to represent the material behavior during contact. As the studied material is virtually divided into elements of square shape, it was proved that the element shape has almost no effect in monotonic loading condition, refer to Ref. (2). After separation of elements and during collision process, this effect becomes much more obvious. As the collision check of irregularly shaped elements is more difficult and time consuming, the element shape during collision is assumed as circle. The following assumptions are adopted for collision springs:

1. The normal spring stiffness is calculated as follows:

$$K_n = \frac{E \cdot d \cdot t}{D} \quad (5)$$

Where "E" is Young's Modulus; t the element thickness; "D" the distance between element centers and "d" the contact distance which is assumed as 10 % of the element size.

2. The shear spring stiffness is assumed 1 % of that of the normal spring. The actual value mainly depends on the studied material type.
3. Normal spring stiffness is assumed constant. This means that compression failure of normal spring is not allowed. During collision of elements in actual cases, part of the energy is dissipated during collision. This effect is represented by adopting different loading and unloading stiffness and this effect will be discussed in the next section.
4. Although the normal contact spring is not allowed to fail, compression failure of distributed springs connecting the elements is allowed instead. This means that the objective of the collision spring is mainly to transmit the stress wave to the other elements.
5. The normal spring is supposed not to have any tensile force. Having some tensile force in the normal spring indicates that elements tend to separate each other. Then, the residual tension and shear forces are redistributed in the next increment.

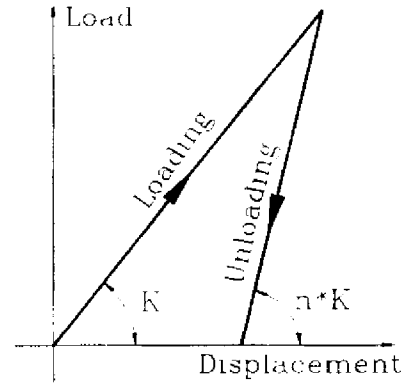


Fig. (2) Load-displacement relation of a contact spring in loading and unloading condition

It should be emphasized that the material models used for representation of collision are approximate. For better representation of material behavior, refer to Ref. (12) and (13).

c) Energy dissipation during collision process

During collision of elements, some of kinetic energy of elements before collision is lost during collision process. The rebound factor (r) is defined as the ratio between the element relative velocity before and after collision. The value of " r " ranges between 0 and 1. Having " r " equals 1.0 means that the relative velocity after collision is the same like before collision and hence, no energy dissipation. While all of the kinetic energy is lost during contact if " r " equals 0. In general, representation of energy dissipation during collision process can be performed by determining the velocity of the elements after collision from the momentum theory and using rebound factor " r ". Although this technique is simple, when it is applied to continuum material like concrete, very small time increment requires to be used to simulate transmission of stress wave due to collision through the other elements. This technique is more suitable for representation of energy dissipation of collision of discontinuous materials.

The following technique is proposed for representation of the energy dissipation during contact. The load-displacement relation of a spring during loading (approaching) and unloading (leaving) are shown in Fig. (2). Assume the factor " n " represents the ratio between the unloading and loading stiffness. The value of " n " should be greater than "1". Having " n " equals 1 means that there is no energy dissipation during contact process while all the kinetic energy is lost if " n " value approaches infinity. The unloading stiffness factor " n " can be correlated easily to the rebound factor " r " by equating the rebound energy of elements in both techniques. This relation is:

$$r = \frac{1}{\sqrt{n}} \quad (6)$$

This indicates that energy dissipation during contact can be simulated by any of these methods. The main advantage using unloading stiffness technique is that the time increment used should be reduced only during the contact of elements. Larger value of time increment can be used after separation.

The calculated velocities before and after collision is checked using the relation shown in Eq. (6) in the following section.

VERIFICATION OF THE NUMERICAL TECHNIQUE

The proposed numerical technique is verified by comparing with theoretical results. The first group of analyses is collision of a free falling element under its own weight with the ground. To check the effect of the unloading stiffness factor (n), a series of analyses are performed using different (n) values, $n=1, 2, 3, 4, 5, 10$. The size of the element as shown in Fig. (3) is $(1 \times 1 \text{ m})$ and it falls from 4.0 m height. The ground is represented by a group of elements at the ground level. Contact springs are set between the element and the ground at the time of collision and removed after separation of elements. Two values of time increment were used, 0.001 (sec) before contact and 0.00001 (sec) during contact. The element thickness is taken as 0.25 m and its density is 2.5 tf/m^3 . The contact spring stiffness is calculated by Eq. (5) to be $5.25 \times 10^5 \text{ tf/m}$. The displacements of the block before and after collision for different unloading stiffness values are shown in Fig. (3). It can be noticed easily that:

1. The obtained displacement values are identical with the theory.
2. The maximum height of the element after rebound is reduced due to energy dissipation. When " n " equals one, no energy dissipation takes place and the element rebound to the original height.
3. The element motion is damped faster when the " n " value is larger. This means that the time required for an element to stop becomes short when " n " is large.

Figure (4) shows the relation between velocity and time. When " n " equals one, the velocity before and after collision are the same. This is equivalent to " r " equals 1. This means that all kinetic energy is recovered after separation of elements. The rebound factor " r " can be calculated easily from element velocities before and after separation. Nearly five values for rebound factor is calculated from each graph. This value is compared with the theoretical one and the results are shown in Fig. (5). Excellent agreement can be observed easily,

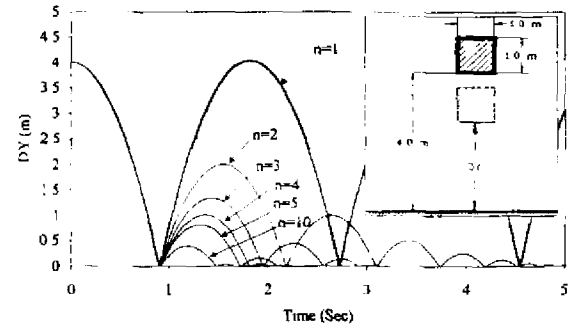


Fig. (3) Time history of displacement of a falling element under its own weight with different unloading stiffness factors

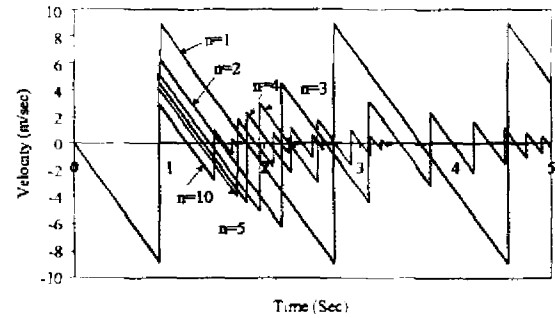


Fig. (4) Time history of velocity of a falling element under its own weight with different unloading stiffness factors

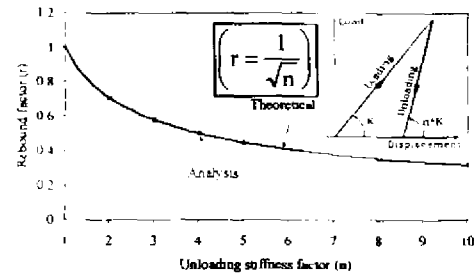


Fig. (5) Relation between calculated and theoretical rebound factor " r " for different unloading stiffness factors " n "

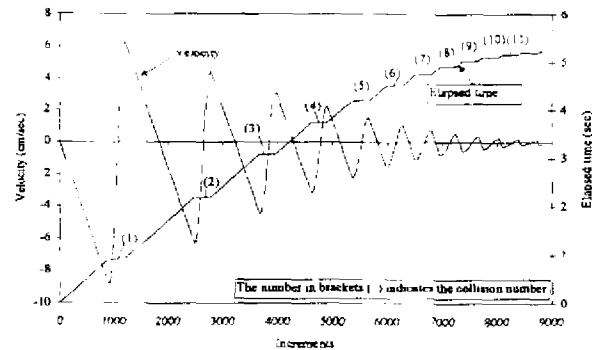


Fig. (6) Changes of velocity components with time in case of " $n=2$ "

Table (1) Comparison between simulated and theoretical contact time of a falling element

Collision number (-th)	1	2	3	4	5	6	7	8
Simulated contact time $DT_s(x 10^5)$	294	294	295	295	295	295	295	297
Error ratio (%)	0.6	0.6	0.9	0.9	0.9	0.9	0.9	1.6

indicating that both techniques are two different ways for representation of energy dissipation during collision.

The elapsed time and the element velocity when "n" equals 2 are shown in Fig. (6). The horizontal axis represents the number of increment. When the elapsed time curve becomes flat, collision occurs and time increment is very small. The main objective of this figure is to show the element behavior during contact process. From Fig. (6), the followings can be noticed:

1. After contact, velocity is reduced gradually till zero and then the direction is reversed.
2. Although the velocity after rebound changes, the contact time "DT" is almost constant. This time is mainly function of the element mass and spring stiffness and can be calculated through Eq. (7), where, "m" is the element mass; "K" the contact spring stiffness and n is the rebound factor. Table (1) shows a comparison between simulated "DT_s" and theoretical "DT_t" contact time. The error is less than one percent till seven successive contacts. The error value increases when the element velocity decreases and the element tends to stop.

$$\frac{\pi}{2} \sqrt{\frac{m}{K}} \left(1 + \frac{1}{\sqrt{n}} \right) \quad (7)$$

The previous example was for only one falling element. As the element is not connected to any other elements, it behaves as a rigid body, i.e. no energy is stored inside the material during collision. To show the energy changes with time, the following example is introduced. This is a block, whose dimensions is (1.0 x 1.0 m), falls from 5.0 m height and it collides with the ground as shown in Fig. (7). The block is divided into 100 square-shaped elements the size of which is (0.1 x 0.1 m). During the analysis, mainly energies are considered: Kinetic energy, potential energy, strain energy inside the block and strain energy stored in the contact springs. The strain energy mainly appears during the contact time and it vanishes after separation of elements. The unloading stiffness factor, n, was taken "1" and "2". The simulation time increment before collision is 0.01 (sec). During the collision process, it is 0.00001 (sec) when "n" equals 1 while it is 0.0001 (sec) when "n" equals 2.

The changes of energy components, when "n" equals 1, are shown in Figs. (7) and (8). From Fig. (7), it can be noticed that the total energy is always constant. The potential energy is reduced when the block is released under its own weight and the kinetic energy increases. Summation of both energies is always constant and equals to the initial energy. Figure (8) illustrates the transfer of different energy components during contact process. When the block touch with the ground, kinetic energy decreases while energy in contact springs and distributed springs increases. The strain energies become maximum when the block stops. When the block starts moving upward, strain energies are reduced while kinetic energy increases. After separation between the block and the ground, the kinetic energy decreases while potential energy increases. In all cases, the summation of all energy components is constant and equals to the initial energy as there is no energy dissipation allowed.

For case when "n" equals 2, the energy distribution results are shown in Figs. (9) and (10). The energy is reduced to the half of the previous value. The calculated and theoretical total energies are almost the same. In each stage, the energy is kept constant till the unloading of the spring force after collision starts. During unloading process, refer to Fig. (10), spring loses half of its energy, because "n" equals 2, and hence, rebound velocity is less than the velocity before collision. The process is repeated accurately till the block stops.

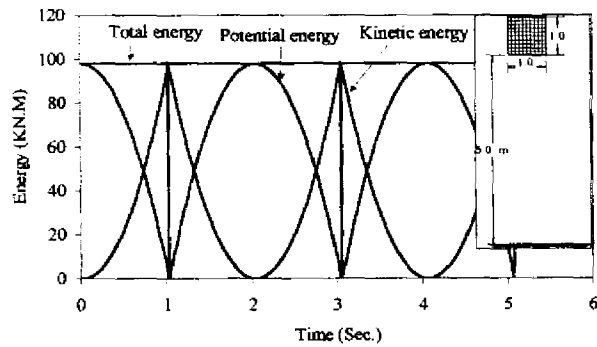


Fig. (7) Changes of kinetic energy, potential energy and total energy with time for a falling block composed of 100 elements under its own weight
"Unloading stiffness factor, $n=1$ "

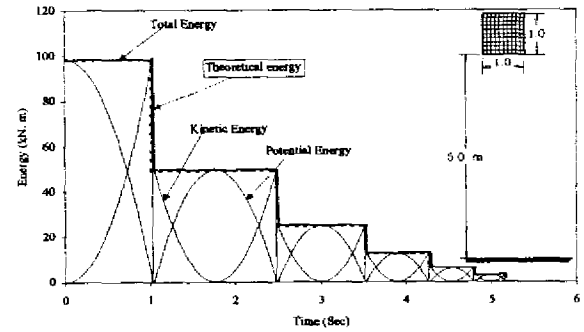


Fig. (9) Changes of kinetic energy, potential energy and total energy with time for a falling block composed of 100 elements under its own weight
"Unloading stiffness factor, $n=2$ "

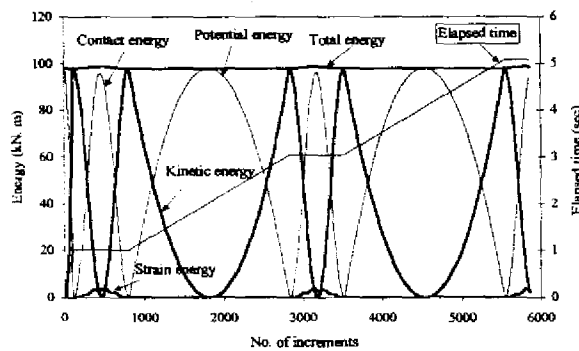


Fig. (8) Changes of energy components and elapsed time with number of increments for a falling block composed of 100 elements under its own weight
"Unloading stiffness factor, $n=1$ "

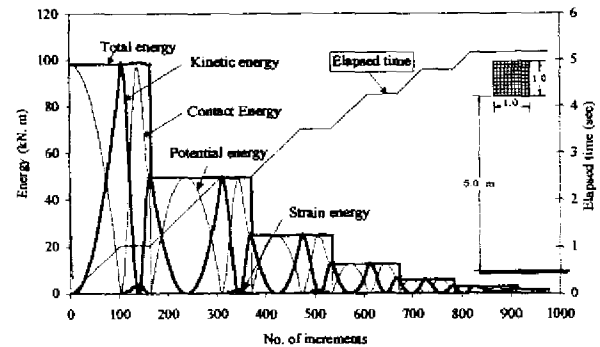


Fig. (10) Changes of energy components and elapsed time with number of increments for a falling block composed of 100 elements under its own weight
"Unloading stiffness factor, $n=2$ "

The previous two analyses show that the transfer of energy components from potential to kinetic to strain energies can be simulated with high accuracy. Moreover, the energy dissipation during collision process can also be simulated without any use of complicated techniques. Although the time increment in both cases is different, accuracy of the simulation did not affected because the time increment used is smaller than the contact time. This indicates that the numerical technique is generally stable and accurate. To simulate collision and/or rebound process accurately, the time increment used requires being, at least, shorter than the contact time, which is function of the mass and contact spring stiffness. Using larger value of time increment leads to inaccurate rebound velocity.

The fourth verification example is for failure of RC frame under falling block. The block and frame dimensions and reinforcement are shown in Fig. (11). The reinforcement arrangement is not symmetrical. The material properties were taken as:

$\sigma_y = 3,600 \text{ kg/cm}^2$, $\sigma_{max} \text{ (reinforcement)} = 5,400 \text{ kg/cm}^2$, $\sigma_c = \text{(not allowed to fail)}$, $\sigma_t = 20.0 \text{ kg/cm}^2$, $E_c = 210 \text{ t/cm}^2$ and $n = 10$. The block weight is 25 tons it falls from five-meter height. The frame is expected to fail, as it is not designed to carry such high impact forces. The two-dimensional analysis is performed using 850 square shaped elements for frame, 100 elements for the falling block and 100 elements for the ground. The time increments used in the simulation are 0.01 (sec) and 0.0001 (sec) before and after collision, respectively. The failure history of the frame, as shown in Fig. (12), can be summarized as follows:

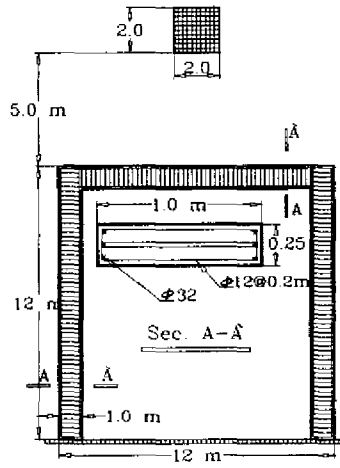


Fig. (11) Shape, dimension and reinforcement details of an RC frame and a falling block

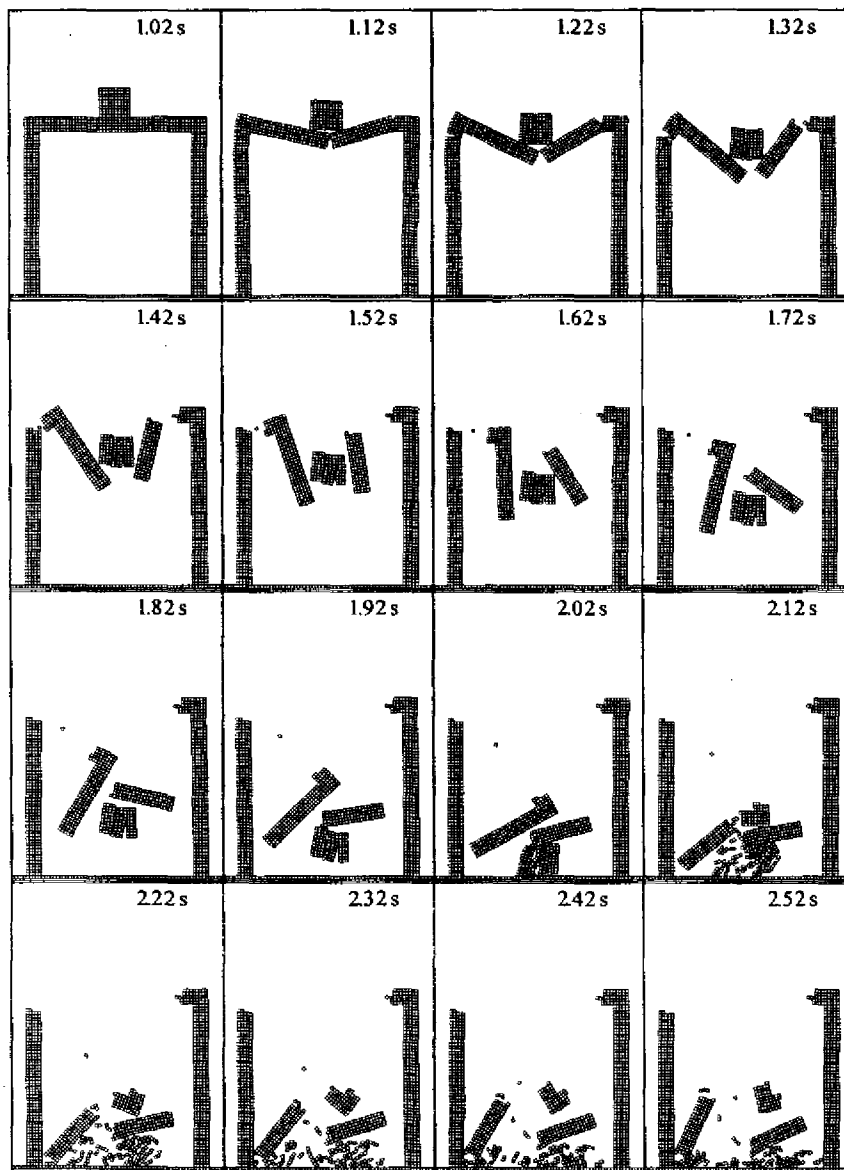


Fig. (12) Failure process of an RC frame attacked by a falling rock

1. The falling block attacks the frame after about 1 second
2. Bending cracks appears first in tensile side at the middle of the beam. Next bending cracks are generated at the connections.
3. The falling block is cracked in the middle because of high collision forces.
4. The reinforcement is cut at the middle of the beam and at connections.
5. The beam is divided into two main rigid parts.
6. The separated parts rotate in the space as a rigid body.
7. The falling block reaches the ground.
8. After collision of the block with the ground and with the failed parts all block elements are cracked because of high normal stress wave propagates through the block elements.
9. Collision between failed structural elements and the rigid block results in separation of the failed elements into two parts.

CONCLUSIONS

Extension of the Applied Element Method to follow collapse behavior of the structure is introduced. A new strategy is introduced to follow the collision behavior of the structural elements during failure. The results obtained by the proposed technique were verified through comparison with theoretical results, and they showed very good agreement. The main conclusions from the previous discussions are:

1. The method is numerically stable and it can be applied to various kind of materials and/or failure phenomenon.
2. No knowledge about fracture and failure behavior of the structure is required before the analysis.
3. The proposed method can follow very large geometrical changes as well as separation of elements without limitations.
4. The CPU time per time increment increases after collision starts. This time is proportional to the number of contacts existing
5. Simple models for concrete, steel and cut of reinforcement are used as the first step in the research. For future study discussing the detailed collapse mechanism of structures, additional effects like buckling of reinforcement bars, separation of concrete cover, compression shear failure and strain rate effect on material properties are needed to be modeled which are not taken into account in the model yet. However, these don't decide the limitation of the capacities of the proposed model; they are material modeling issues and any type of material models can be used in the proposed model.
6. It is very difficult, or practically impossible, to follow such behavior using the methods in which the material is continuous, like FEM and BEM. With the methods failure analysis is still restricted to cases where failure patterns is known before the analysis.
7. Among the conventional numerical models, the EDEM is one of the few models which can simulate such collapse behavior. The main advantage of the proposed method compared to the EDEM is that the time increment can be enlarged before collision starts. In EDEM, the time increment is restricted to a certain small value, which is function of the material type and element size. It can not be enlarged even before collision starts. In the proposed method, longer time increment can be used before collision; it is up to the objective phenomena. Small time increment, which are still much larger than those used in DEM, is needed only during collision process or in case of impulsive dynamic problems.

REFERENCES

1. Meguro K. and Tagel-Din H.: A new efficient technique for fracture analysis of structures, *Bulletin of Earthquake Resistant Structure*, No. 30, pp. 103-116, 1997.
2. Meguro K. and Tagel-Din H.: A new simplified and efficient technique for fracture behavior analysis of concrete structures, *Proceedings of the Third International Conference on Fracture Mechanics of Concrete and Concrete Structures (FRAMCOS-3)*, Gifu, Japan, Oct. 1998.

3. Tagel-Din H. and Meguro K.: Consideration of Poisson's ratio effect in structural analysis using elements with three degrees of freedom, *Bulletin of Earthquake Resistant Structure*, No. 31, pp. 41-50, 1998.
4. Meguro K. and Tagel-Din H.: A new simple and accurate technique for failure analysis of structures, *Bulletin of Earthquake Resistant Structure*, No. 31, pp. 51-61, 1998.
5. Meguro K. and Tagel-Din H.: Simulation of buckling and post-buckling behavior of structures using applied element method, *Bulletin of Earthquake Resistant Structure*, No. 32, 1999
6. Meguro K. and Hakuno M.: Application of the extended distinct element method for collapse simulation of a double-deck bridge, *Structural Eng./Earthquake Eng.*, Vol. 10. No. 4, 175s-185s., Japan Society of Civil Engineers, 1994.
7. Kusano N., Aoyagi T., Aizawa J., Ueno H., Morikawa H. and Kobayashi N.: Impulsive local damage analysis of concrete structures by the distinct element method, *J. of Nuclear Engineering and Design*, No. 138, pp. 105-110, 1992.
8. Amadei B., Lin C. and Dwyer J.: Recent extensions to the DDA method, *Proc. of 1st Int. Forum on Discontinuous Deformation Analysis (DDA)*, Berkley, California, Ed. Salami & Banks (1996).
9. Chopra K.: *Dynamics of structures, Theory and applications to earthquake engineering*, Prentice Hall, 1995.
10. William H.: *Numerical Recipes in Fortran 77*, Cambridge University Press, New York, 1996.
11. Bar P.: *Guidelines for the design and assessment of concrete structures subjected to impact*, United Kingdom Atomic Energy Authority, Safety and Reliability Directorate, SRD R 439, 1987.
12. CEB Comite Euro-International Du Beton: *Concrete structures under impact and impulsive loading*, Report No. 187. Dubrovnik, 1998.
13. Taylor L.M. and Preece D.S.: Simulation of blasting induced rock motion using spherical element method, 1st U.S. Conf. on DEM, Eds. G.G. W. Mustoe, M. Henriksenksen and H.P. Huttelmaier, 1989.